Human lymphatic pumping measured in healthy and lymphoedematous arms by lymphatic congestion lymphoscintigraphy

S. Modi[1,3], A. W. B. Stanton[1,3], W. E. Svensson[3], A. M. Peters[4], P. S. Mortimer[1] and J. R. Levick[2]

[1]*Cardiac and Vascular Sciences (Dermatology) and* [2]*Basic Medical Sciences (Physiology), St George's Hospital Medical School, University of London, London SW17 0RE, UK*

[3]*Nuclear Medicine, Hammersmith Hospital, London W12 0HS, UK*

[4]*Nuclear Medicine, Royal Sussex County Hospital, Brighton BN2 5BE, UK*

Axillary surgery for breast cancer partially obstructs lymph outflow from the arm, chronically raising the lymphatic smooth muscle afterload. This may lead to pump failure, as in hypertensive cardiac failure, and could explain features of breast cancer treatment-related lymphoedema (BCRL) such as its delayed onset. A new method was developed to measure human lymphatic contractility non-invasively and test the hypothesis of contractile impairment. ^{99m}Tc-human IgG (Tc-HIG), injected into the hand dermis, drained into the arm lymphatic system which was imaged using a gamma-camera. Lymph transit time from hand to axilla, $t_{transit}$, was 9.6 ± 7.2 min (mean ± S.D.) (velocity 8.9 cm min^{-1}) in seven normal subjects. To assess lymphatic contractility, a sphygmomanometer cuff around the upper arm was inflated to 60 mmHg (P_{cuff}) before ^{99m}Tc-HIG injection and maintained for $>> t_{transit}$. When P_{cuff} exceeded the maximum pressure generated by the lymphatic pump (P_{pump}), radiolabelled lymph was held up at the distal cuff border. P_{cuff} was then lowered in 10 mmHg steps until ^{99m}Tc-HIG began to flow under the cuff to the axilla, indicating $P_{pump} \geq P_{cuff}$. In 16 normal subjects P_{pump} was 39 ± 14 mmHg. P_{pump} was 38% lower in 16 women with BCRL, namely 24 ± 19 mmHg ($P = 0.014$, Student's unpaired t test), and correlated negatively with the degree of swelling (12–56%). Blood radiolabel accumulation proved an unreliable measure of lymphatic pump function. Lymphatic congestion lymphoscintigraphy thus provided a quantitative measure of human lymphatic contractility without surgical cut-down, and the results supported the hypothesis of lymphatic pump failure in BCRL.

(Received 13 February 2007; accepted after revision 10 June 2007; first published online 14 June 2007)

Corresponding author A. W. B. Stanton: St George's Hospital Medical School, University of London, Cranmer Terrace, London SW17 0RE, UK. Email: astanton@sgul.ac.uk

Breast cancer treatment-related lymphoedema (BCRL) or 'surgical elephantiasis' (Halsted, 1921) is a chronic, incurable and debilitating swelling of the arm resulting from the removal of axillary lymph nodes and often axillary radiotherapy during breast cancer treatment. The heavy, swollen arm causes functional and psychological morbidity and is prone to infection, e.g. cellulitis (Stewart & Treves, 1948; Velanovich & Szymanski, 1999; Hack *et al.* 1999). Around 42 000 women per year are diagnosed with breast cancer in the UK (www.cancerresearchuk.org), and BCRL develops in ∼25% of those undergoing axillary node clearance (Mortimer *et al.* 1996; Schunemann & Willich, 1997). Even when surgery is limited to the removal of a single, 'sentinel' lymph node (first node downstream of tumour), the incidence of BCRL is surprisingly high, at approximately 6% (Blanchard *et al.* 2003; Mansel *et al.* 2006).

Axillary lymph node removal and radiotherapy are clearly the initiating factors in BCRL but the complex temporal and spatial pathophysiology remains inadequately explained. The simplest view is that obstruction of the axillary drainage routes causes interstitial fluid to accumulate in the arm. This 'stopcock' hypothesis fails, however, to explain the unusual temporal and spatial features of BCRL. Specifically (i) some patients develop BCRL after a single sentinel node biopsy, yet many do not despite more extensive substantial axillary clearance. (ii) The onset of chronic swelling is usually months or years after the axillary insult, with no obvious precipitating event (Mortimer *et al.* 1996). (iii) The

 DOI: 10.1113/jphysiol.2007.130401

spatial distribution of swelling along the arm is often non-uniform (Modi *et al.* 2005); moreover the hand is sometimes spared and shows no depression of the lymph drainage rate constant, despite drainage to the same damaged axilla (Stanton *et al.* 2001, 2006). By contrast, the lymph drainage rate constant is depressed in swollen hands and in both the subcutis and muscle of swollen forearms (Stanton *et al.* 2001, 2003, 2006; Pain *et al.* 2004*b*). The axillary stopcock hypothesis does not adequately explain the above anomalies.

It is generally accepted that axillary node extirpation raises the resistance to lymph drainage from the arm, and hence raises pressure in the lymphatics. For example, lymphangiography in BCRL shows dilated tortuous vessels, axillary lakes, and leaked extra-lymphatic contrast medium in the upper arm and axilla (Feldman *et al.* 1966; Clodius, 1977). This led us to consider the possible effect of a chronically raised afterload on smooth muscle function in the lymphatic walls. The main lymphatic vessels (but not the initial lymphatic capillaries) show rhythmic contractions and actively pump lymph centrally, aided by valves. The lymphatic stroke volume and output decline, however, above a distending pressure of 10 cmH_2O in isolated bovine lymphatics, or 18–26 cmH_2O in conscious sheep, despite increased contraction frequency (McGeown *et al.* 1987; review, Levick & McHale, 2002). Such observations led us to propose the hypothesis of chronic pump failure in BCRL resulting from a chronically raised afterload, as in hypertensive cardiac failure (Stanton *et al.* 2003, 2006; Modi *et al.* 2005). If lymphatic contractility declines slowly and progressively, a tipping-point will eventually be reached where lymph drainage rate no longer matches capillary filtration rate, precipitating the onset of swelling in the drainage territory of the failing lymphatics. The (variable) period required for the critical degree of failure could explain the variable delay in onset of BCRL. If the constitutionally weakest lymphatic collector vessels fail first, swelling would be localized to their drainage territory, offering a rational explanation for the regionality paradox.

Unfortunately, there were no non-invasive methods for measuring lymphatic pump force in humans. Methods such as fluorescence microlymphography and radio-labelled protein clearance from an interstitial depot assess primarily the function of the non-contractile initial lymphatic capillaries (Modi *et al.* 2007). γ-Camera imaging of limb lymphatics after take-up of labelled interstitial macromolecules is qualitative (Mellor & Mortimer, 2004). Direct cannulation of leg lymphatics has shown that normal human leg collector vessels are capable of pumping to ~45 mmHg (Olszewski & Engeset, 1980), but this approach requires surgical cut-down and is not ethical with BCRL patients. The closest previous approach to a non-invasive method was provided by a study of simulated snake envenomation by Howarth *et al.* (1994). They gave subcutaneous injections of a radio-tracer at the wrist and found that a bandage pressure of 40–70 mmHg was required to prevent the lymphatic transport of the tracer to the axilla. The method developed here to measure human arm lymphatic contractile force is a development of their approach. ^{99m}Tc-human immunoglobulin (^{99m}Tc-HIG), a labelled native protein (cf. traditional non-native agents such as sulphur colloid), was injected intradermally. Since dermal lymphatic density is high (Stanton *et al.* 1999*b*), this route of injections rapidly fills the arm lymphatics, enabling them be imaged by a γ-camera (Pain *et al.* 2003; O'Mahony *et al.* 2004). A congestion cuff was then used to probe the occluding pressure that lymphatic contraction could overcome. In the current study we used this new method to test the hypothesis that lymphatic collector pump force is weakened in BCRL.

Methods

Seven healthy subjects (4 women, 3 men) aged 52 ± 10 (S.D.) years underwent the 'uncuffed healthy subject protocol' (see below) and 16 healthy subjects (11 women, 5 men) aged 54 ± 6 years underwent the 'cuffed healthy subject protocol'. Subjects taking drugs likely to affect smooth muscle, such as Ca^{2+} channel antagonists and adrenoceptor agonists/antagonists, were excluded. Sixteen women with BCRL aged 60 ± 8 years underwent the 'cuffed BCRL protocol' (see below). Patients with recurrent breast cancer, heart disease, hypertension, or taking Ca^{2+} channel antagonists or adrenoceptor agonists/antagonists, were excluded. All had developed ipsilateral (i.e. on the same side as the surgery) BCRL at 2.3 ± 4.5 years (0–216 months) after axillary surgery for unilateral breast cancer (Table 1). Oedema had been present for 6.4 ± 6.2 years (7–234 months) in the dominant arm ($n = 8$) or non-dominant arm ($n = 8$) (Table 1). Fourteen patients routinely wore a compression sleeve but not on the study day. The study was approved by the Hammersmith Hospitals NHS Trust Research Ethics Committee and by the Administration of Radioactive Substances Advisory Committee of the UK (ARSAC). All subjects gave informed, written consent and the studies conformed to the standards set by the *Declaration of Helsinki*.

Measurement of arm and hand volumes

Arm volume was measured between identical points for each pair of arms. The volume between the ulnar styloid process (wrist) and anterior axillary fold (upper arm) was measured by an opto-electronic limb volumeter (Perometer 350S, Pero-System Messgeräte GmbH, Wuppertal, Germany) as validated previously (Stanton *et al.* 1997; Stanton *et al.* 2000). For the proximal 4–8 cm of the upper arm, beyond the technical

Table 1. Details of patients, breast cancer treatment and breast cancer-related lymphoedema (BCRL)

									BCRL		
Patient no.	Age (yrs)	Ipsilateral arm	Hand swelling	Operation*	Lymph node status†	Chemo-therapy	Radio-therapy	Hormonal treatment	Delay‡ (months)	Duration (months)	%#
1	53	R	Y	WLE	0/5	N	Y	Y	18	71	32.0 (41.7)
2	51	R	Y	WLE	0/14	Y	Y	Y	60	72	14.8 (28.8)
3	62	R	Y	Mast	18/42	Y	Y	N	12	44	27.4 (37.2)
4	63	L	Y	WLE	0/6	N	Y	Y	6	20	16.7 (11.3)
5	77	L	N	WLE	0/19	N	Y	Y	0	204	38.5 (13.6)
6	56	R	Y	Mast	2/5	Y	Y	N	0	152	38.3 (66.4)
7	66	R	N	Mast	0/24	N	N	Y	45	7	12.1 (15.9)
8	58	R	N	Mast	0/28	N	N	Y	24	54	14.6 (17.2)
9	61	L	N	Mast	0/15	N	N	Y	0	48	12.1 (11.0)
10	66	L	Y	WLE	13/15	Y	Y	Y	13	14	36.3 (43.9)
11	50	L	Y	Mast	0/10	N	Y	N	216	15	56.4 (68.0)
12	60	L	N	WLE	Unknown	N	Y	Y	0	168	22.3 (24.0)
13	66	L	Y	Mast	0/16	Y	Y	Y	36	234	36.8 (69.3)
14	57	L	Y	WLE	0/16	N	Y	Y	0	25	17.2 (21.1)
15	49	R	N	WLE	Unknown	N	Y	Y	0	212	11.8 (18.0)
16	67	L	Y	WLE	0/26	N	Y	N	12	83	35.3 (44.3)

R, right; L, left; Y, yes; N, no; *WLE, wide local excision; Mast, simple mastectomy. †Number of lymph nodes positive for tumour/number excised. ‡Interval between surgery and onset of BCRL. #Percentage increase in total arm volume relative to opposite side (% increase in forearm volume in parentheses). Post-operative complications: seroma (accumulation of lymph in the axilla) in patients 10 and 16; arm swelling (resolving in < 2 months) in patients 2, 5, 8 and 9; cording (axillary web syndrome, believed to be caused by lymphangitis; a tightness experienced in the axilla or down the arm upon abduction and external rotation; a fine cord can be seen or palpated or cause guttering on the overlying skin) in patients 2, 4, 6, 7, 8, 9, 12 and 14. Patient 10 was left-handed, all others were right-handed.

limit of the Perometer, circumferences were measured with a flexible tape-measure at 4 cm intervals and volume calculated by the truncated cone formula: volume (ml) $= \Sigma(X^2 + Y^2 + XY)/3\pi$, where X is the first circumference measurement and Y is the circumference 4 cm proximally. Hand volume was measured by water displacement (mean of 3; Stanton *et al.* 2000).

Comparison of brachial artery blood pressure measurement using a Riva-Rocci cuff on swollen and non-swollen side

Brachial artery blood pressure (BP) was measured by auscultation in each arm using a mercury sphygmomanometer and Riva-Rocci congestion cuff. The comparison tested an inherent assumption of the lymphatic congestion method, namely that the transmission of the occluding pressure from the cuff to the deep tissues was not impaired in the BCRL arms. The cuff size was tailored to the size of the upper arm. The dimensions of each cuff and its air bladder are shown in relation to the mid upper arm circumference in Table 2. Mean blood pressure in each arm was calculated as diastolic pressure $+ {}^1/_3$ pulse pressure. In all subjects the diastolic blood pressure was ≥ 60 mmHg, the maximum cuff pressure used in lymphatic arrest studies.

Table 2. Tailoring of cuff dimensions to arm size

Cuff	Length (cm)	Width (cm)	Air bladder length (cm)	Air bladder width (cm)	Range of upper arm circumfs (cm)
Std	46.3	14.3	22.2	11.3	27.4–29.7
1	53.0	14.3	29.5	13.0	29.7–38.2
2	57.3	14.3	36.5	13.0	38.9–41.2
3	61.5	14.3	40.0	13.0	$>$ 41.2

Size of standard adult size (Std) and custom-made pressure cuffs (1–3) and size of corresponding air bladders were adjusted according to the ipsilateral mid upper arm circumference, in accordance with clinical practice, to prevent the attenuation of pressure transmission in large limbs.

Gamma-Camera imaging of arm

The subject was supine for imaging of the arm. The two heads of a double-headed γ-camera (E.CAM 180 double-headed, rectangular field of view camera with low-energy, high-resolution collimator; Siemens, PA, USA) were positioned 31 ± 3 cm apart to provide anterior and posterior images of radiolabel-filled arm lymphatic (Fig. 1). The image included all the axillary and supraclavicular nodes, the upper arm lymphatics, and as much of the forearm as possible. The arm contour was traced onto the detector surface using a cobalt-57 pen

and recorded, to ensure that the unfilled axilla and arm were in the field of view. Background radioactivity was recorded by a 3 min acquisition prior to tracer injection. Room temperature was $23.2 \pm 0.7^{\circ}$C.

Radiolabelled macromolecular marker for lymph and dose of radiation

A radiolabelled polyclonal human immunoglobulin, technetium-99m-labelled human IgG (^{99m}Tc-HIG) (TechneScan HIG, Mallinckrodt Medical B.V., Petten, The Netherlands) was prepared by Mallinckrodt Pharmacy Services (University College Hospital, London). Radiochemical purity (percentage bound label) was assayed by the radiopharmacy laboratory using gel chromatography (Sephadex PD_{10}, exclusion molecular mass > 5000 Da) and the purity of the injected product was $\geq 95\%$ bound ^{99m}Tc. This radiopharmaceutical is readily taken up into the lymphatic system following dermal injection (O'Mahony *et al.* 2004). The administered activity ($\sim$10 MBq ^{99m}Tc, see Protocol) gave an effective dose of 0.15 mSv.

Uncuffed protocol, healthy subjects

Measurements of the lymphatic transit time from hand to axilla (t_{transit}) in the absence of external lymphatic compression were used to plan the duration of occlusion in cuffed studies. Either arm was studied. With the subject supine, the tracer was injected intradermally between the 2nd and 3rd metacarpophalangeal joints of the clenched fist, because this route produces the best images of the arm lymphatic (O'Mahony *et al.* 2004). Fifty microlitres of ^{99m}Tc-HIG (25 μg HIG, activity 9 ± 3 MBq) was injected slowly ($\sim$1 min) through a steel 36 gauge needle (external diameter 0.2 mm; Unimed S.A., Lausanne, Switzerland) inserted horizontally facing the wrist. The intradermal location was confirmed by resistance to injection (cf. subcutis), blanching and a visible raised bleb. A dynamic image sequence of 40 frames over the arm and axilla was then acquired over 2 h (3 min per frame), followed by a 3 min static acquisition over the hand to determine how much radioactivity remained in the injection depot. The dominant arm was studied in five subjects and the non-dominant arm in two subjects. Blood samples were taken from the opposite arm (see below). When imaging was complete, the subject stood up, walked to the waiting area and sat until blood sampling was complete.

Analysis of labelled lymph transit in uncuffed protocol

Three regions of interest (ROI) were examined on each arm image, namely the regions distal to (ROI 1), beneath (ROI 2), and proximal to (ROI 3) the cuff location used in cuffed protocols. ROI 3 corresponded to the axillary region. After correction for background activity and radioactive decay, the counts per min (CPM) of each ROI were plotted against time. The time at which the counts in the proximal, axillary ROI rose above background was defined as the lymphatic transit time, t_{transit}. Lymph velocity in uncuffed studies was measured between the depot and ROI 3 (axilla) and calculated as the distance divided by

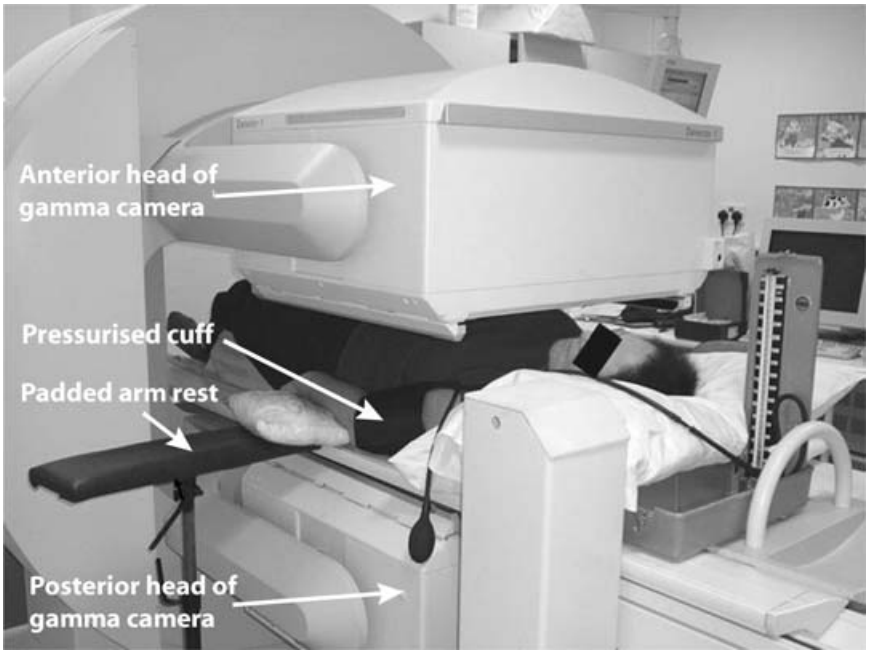

Figure 1. Patient with BCRL under Gamma-camera during cuffed protocol
The left lymphoedematous arm has a cuff around the upper arm which, at high inflation pressures, occludes the underlying lymphatic collectors. A cannula has been inserted into a vein in the right antecubital fossa for blood sampling (not visible).

the time taken for counts to reach ROI 3. The amount of ^{99m}Tc-HIG in the initial depot was calculated from the difference between injection syringe activity in CPM before and after the injection, corrected for decay. Using this value, the CPM in each ROI could be normalized as a fraction of the injected CPM.

Cuffed protocol, healthy subjects

The pressure generated by the contractile activity of occluded lymphatic collectors, P_{pump}, was measured in 14 dominant and 2 non-dominant normal arms. In three of the subjects the individual $t_{transit}$ values were known from the previous uncuffed protocol and these earlier values were compared with $t_{transit}$ obtained in the presence of the cuff to establish that the cuff pressure of 60 mmHg effectively occluded lymph flow. A standard, adult size sphygmomanometer cuff (Accoson, London, UK) was wrapped around the upper arm with the bladder anteromedially, and connected to a standard Accoson mercury sphygmomanometer. This was inflated by hand and maintained at 60 mmHg from 2 min before intradermal ^{99m}Tc-HIG injection in the hand (see above). The initial occluding cuff pressure, P_{cuff}, was less than diastolic arterial pressure, did not cause any paraesthesia or numbness and was well tolerated. At 30 min after ^{99m}Tc-HIG injection, i.e. at a time $>> t_{transit}$, the cuff pressure was reduced by 10 mmHg to 50 mmHg for 15 min. Thereafter P_{cuff} was reduced in 10 mmHg steps at 15 min intervals. The cuff was disconnected when 0 mmHg was reached (105 min) and removed altogether at ∼130 min. The arm lymphatic imaging protocol and blood sampling protocol (see below) were as for the uncuffed protocol. The value of P_{cuff} at which ^{99m}Tc-HIG first passed under the cuff was taken as the measure of P_{pump}. When imaging was complete, the subject stood up and then sat in the waiting area.

Cuffed protocol, BCRL patients

The above protocol was carried out on the 16 patients with BCRL described in Table 1. The cuff size was tailored to the size of the upper arm (Table 2).

Analysis of cuffed protocol images; criteria for P_{pump}

The progressive accumulation of ^{99m}Tc-HIG at the distal border of the cuff and absence of activity under the cuff at times greater than $t_{transit}$ demonstrated that the cuff effectively prevented lymph flow from forearm to axilla. The highest cuff pressure at which ^{99m}Tc-HIG passed under the cuff into the proximal, axillary region (ROI 3) was taken to equal the highest lymph pressure generated by obstructed, contracting arm lymphatics, P_{pump}. Sub-cuff transmission was assessed by inspection initially (Figs 2*A* and 3*A*) and confirmed by quantitative analysis of CPM in the three ROIs (Figs 2*B* and 3*B*).

Lymph velocity in cuffed studies was measured between the depot and cuff distal border and calculated as the distance divided by the time taken for counts to reach the cuff.

Arrival of radiolabel in blood pool

Interstitial macromolecules such as ^{99m}Tc-HIG are cleared principally by the lymphatic system. Therefore, after an initial time lag caused by the lymphatic transit time, the rate of accumulation in blood, J_{tracer}, should in principle be a quantitative measure of lymphatic volume pumping in the uncuffed arm (Pain *et al.* 2002, 2003, 2004*a*,*b*). To assess the time lag and J_{tracer}, antecubital venous blood was sampled from the opposite, non-injected arm during the uncuffed and cuffed protocols. Three baseline 1.5 ml samples were collected in EDTA tubes before the radiolabel injection, then sampling was continued at 2 min after injection and every 5 min for 1 h, followed by every 10 min to 2 h. Two final blood samples were taken at $2^1/_2$ h and 3 h post-injection, after the subject had moved around and sat in the waiting room. One millilitre of whole blood was pipetted into glass counting tubes and counted for 5 min per sample in an automated γ-counter (PerkinElmer Wallac Wizard 1480; Ametek, Wokingham, UK). To determine the amount of radioactivity in the total blood pool, the activity per millilitre was multiplied by total blood volume, which was estimated by a nomogram based on age, sex and weight. Blood pool activity (Bq) was normalized as a percentage of initial depot activity (Bq). The latter was calculated from the difference between injection syringe activity (Bq) before and after the ^{99m}Tc-HIG injection, corrected for decay. J_{tracer} was calculated by linear regression analysis of the mass *versus* time plot for each individual.

Assessment of free ^{99m}Tc in blood

The unexpectedly early appearance of radiolabel in blood (see Results) raised concerns over the stability of ^{99m}Tc binding to HIG *in vivo*. To assess free label in the blood samples, protein-bound radioactivity was precipitated out using trichloroacetic acid (TCA) (Andrews & Milne, 1977). Two millilitre blood samples taken 2 min, 90 min and 180 min after depot injection were centrifuged (5 min, 1000 *g*) and 1 ml plasma transferred to fresh glass tubes containing 1.5 ml 5% TCA. After re-centrifugation (5 min, 1000 *g*) the supernatant was transferred to a counting tube. A further 2.5 ml 5% TCA was added to the pellet and mixed well to resuspend it. This was re-centrifuged and the supernatant transferred to a second counting tube. The pellet was dissolved in 2.5 ml of 2 M sodium hydroxide and transferred to a third counting tube. The

tubes were counted in a γ well counter set for ^{99m}Tc. The counts in all three tubes were corrected for dead time, decay and background radioactivity. Counts from the three tubes were added and counts in the pellet tube (bound counts) expressed as a percentage of the total counts.

Statistical analysis

Results are presented as the mean ± standard deviation (S.D.) unless stated otherwise, followed by the range in brackets where appropriate. Student's paired, unpaired and one-sample *t* tests were used to compare differences between groups. Regression, correlation (*r*) and one-way analysis of variance were as implemented in GraphPad Prism (GraphPad Software, CA, USA). Differences were considered significant if $P \leq 0.05$.

Results

Magnitude of the lymphoedema

The swollen arm volume in BCRL patients averaged 3165 ± 991 ml, which was 26.4 ± 13.2% (11.8–56.4%) bigger than the contralateral arm (2464 ± 677 ml; $P < 0.0001$, $n = 16$, Student's paired *t* test), and likewise bigger than the arms of the healthy subjects (dominant arm 1927 ± 527 ml, non-dominant arm 1902 ± 564 ml; dominant *versus* non-dominant, $P = 0.11$, $n = 23$, Student's paired *t* test). In 9 of the 16 BCRL patients the hand was clinically swollen. Hand volume for all patients ($n = 16$) averaged 360 ± 61 ml ipsilaterally and 327 ± 52 ml contralaterally. For the nine patients with clinically swollen hands, the swollen hand volume, 348 ± 66 ml exceeded the non-swollen hand volume,

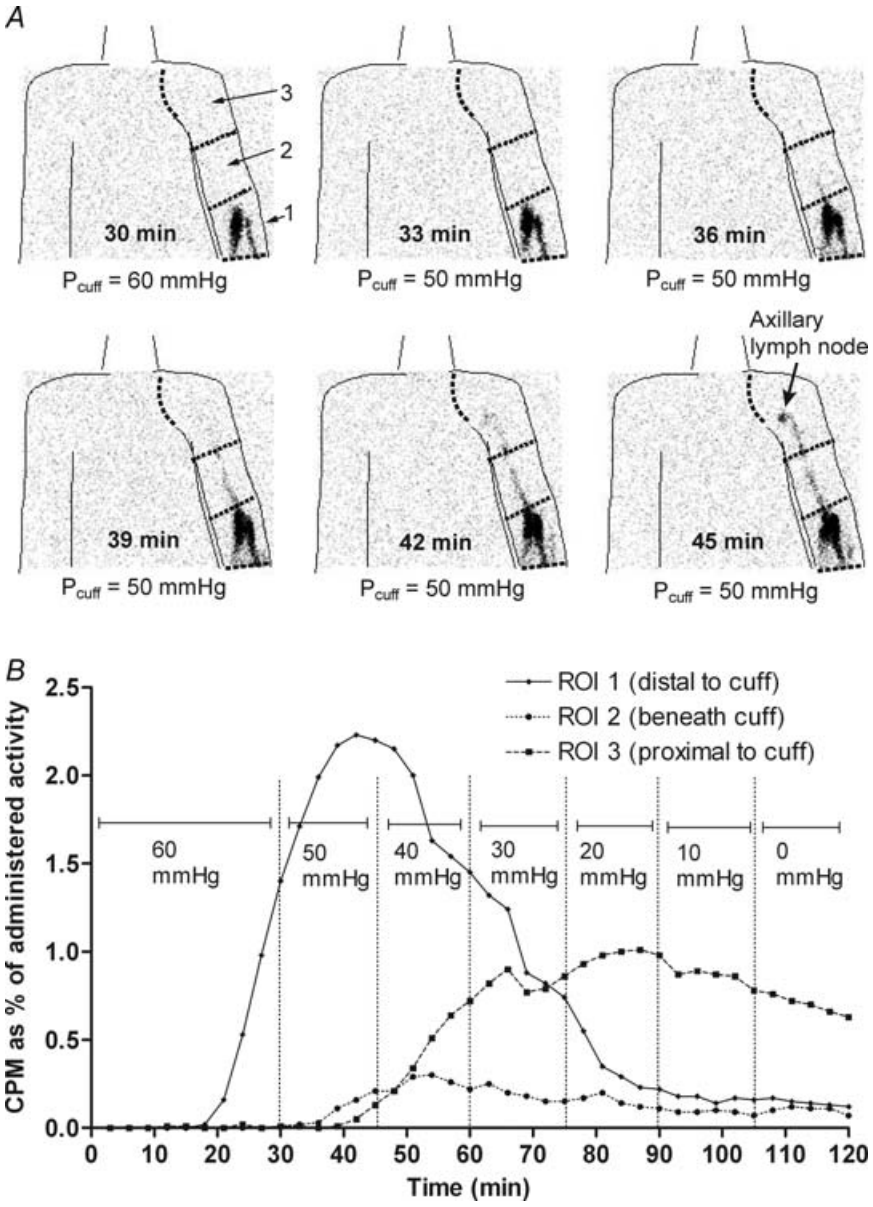

Figure 2. Gamma-Camera results from a normal left arm of a healthy volunteer during lymphatic congestion
A, selected sequence from scan images (anterior view). Regions of interest (ROI) 1, 2 and 3 are shown on the left arm (right side of each image); ROI 2 corresponded to the position of the congestion cuff. At 60 mmHg cuff pressure (P_{cuff}), ^{99m}Tc-HIG was retained distal to the cuff (30 min post-injection). When P_{cuff} was reduced to 50 mmHg, ^{99m}Tc-HIG began to travel under the cuff (36 min), reaching the proximal border of the cuff at 39 min and an axillary lymph node by 45 min. P_{pump} was ~50 mmHg. *B*, region of interest (ROI) analysis, same subject as in *A*. Counts per minute (CPM) were measured in the distal (continuous line), sub-cuff (long-dashed line), and proximal (axillary) (short-dashed line) ROIs in 40 sequential frames and plotted as percentage of administered counts. P_{cuff} is marked for each time interval between the vertical lines. A rise in CPM above background in the proximal, axillary ROI at 39 min ($P_{cuff} = 50$ mmHg) indicated $P_{pump} \geq 50$ mmHg and < 60 mmHg.

316 ± 54 ml, by $10.9 \pm 10.9\%$ (4.6–37.5%) ($P = 0.01$). For those without hand swelling, the ipsilateral and contralateral hand volumes were 330 ± 69 ml and 328 ± 66 ml, respectively ($n = 7$).

Transmission of occluding cuff pressure to deep tissues in swollen *versus* non-swollen arm

In BCRL patients the brachial artery blood pressure measured in the swollen arm, $136 \pm 17/78 \pm 8$ mmHg (systolic/diastolic), was almost identical to that measured in the contralateral non-swollen arm, $135 \pm 17/77 \pm 9$ mmHg (Fig. 4). The between-arm difference in mean blood pressure (contralateral minus ipsilateral) was 0.6 ± 3.3 mmHg ($P = 0.40$, $n = 16$, Student's paired t test). The presence of swelling thus had no significant effect on the transmission of an occluding pressure from the cuff to the deep tissues. Brachial arterial pressure in the healthy subjects was $126 \pm 23/76 \pm 11$ mmHg. All subjects participating in cuffed studies had a diastolic pressure of ≥ 60 mmHg, the highest cuff pressure in the protocol.

Lymph transit from hand to axilla in uncuffed studies

The hand-to-axilla velocity of the lymph radiolabel averaged 8.9 ± 5.8 cm min^{-1} ($n = 7$) in normal, uncuffed subjects. The time interval between depot injection and

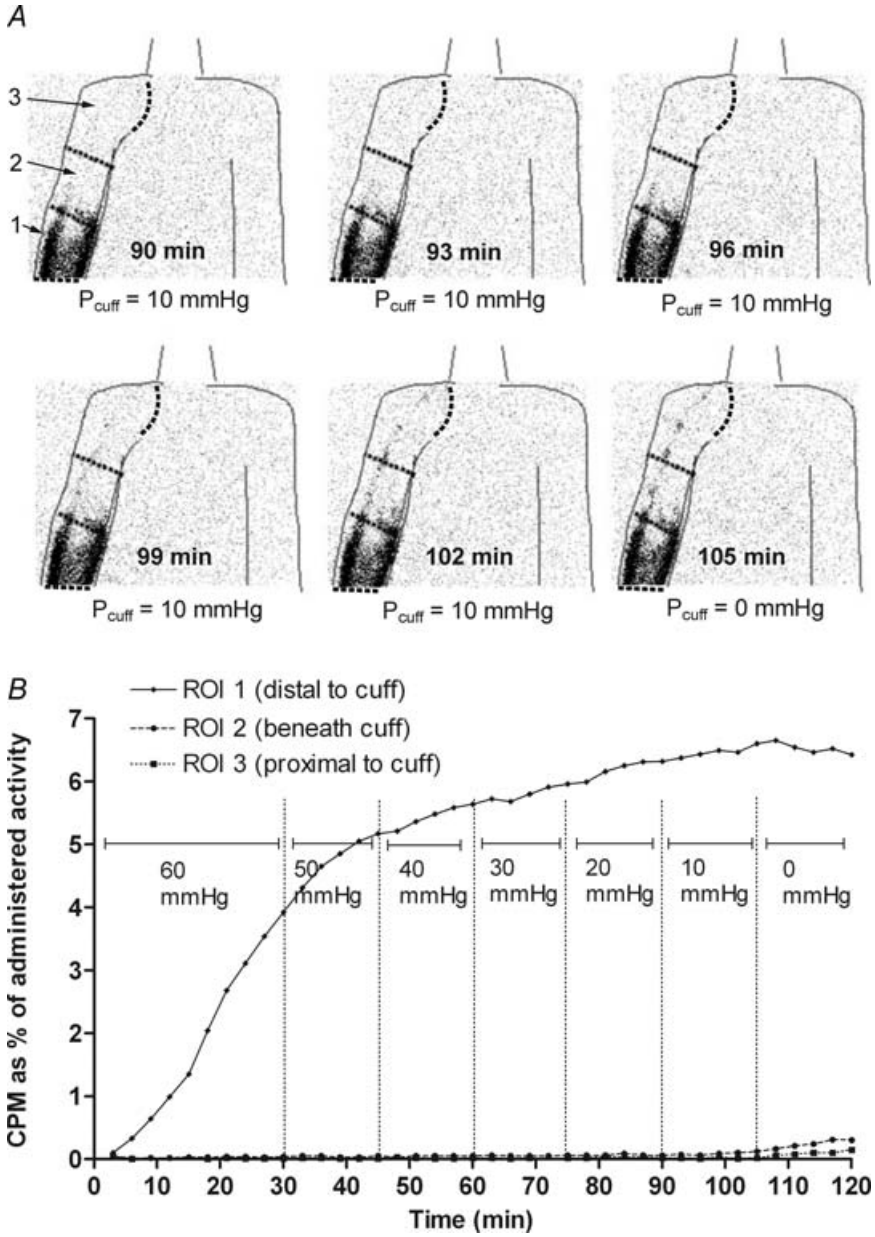

Figure 3. Gamma-Camera results from a lymphoedematous right arm (patient 15, Table 1, and 18% forearm swelling) during lymphatic congestion
A, selected sequence from scan images (anterior view). Regions of interest (ROI) 1, 2 and 3 are shown on the right arm (left side of each image); ROI 2 corresponded to the position of the congestion cuff. Dermal backflow was present at cuff pressures > 10 mmHg. When P_{cuff} was reduced from 20 mmHg to 10 mmHg (90 min post-injection), ^{99m}Tc-HIG began to creep under the distal cuff margin (lower dotted line), reaching the proximal border at 99 min and an axillary lymph node at 105 min ($P_{cuff} = 0$ mmHg). *B*, region of interest (ROI) analysis, same BCRL patient as in *A*. Counts per minute (CPM) were measured in the distal (continuous line), sub-cuff (long-dashed line), and proximal (axillary) (short-dashed line) ROIs in 40 sequential frames and plotted as percentage of administered counts. P_{cuff} is marked for each time interval between the vertical lines. A rise in counts above background in the proximal, axillary ROI (ROI 3) at 99 min ($P_{cuff} = 10$ mmHg) indicated $P_{pump} \geq 10$ mmHg and < 20 mmHg. The early rise in counts in ROI 1 (distal to cuff) compared with the cuffed healthy subject in Fig. 2*B* is accounted for by dermal backflow in the lymphoedematous arm.

Table 3. Comparison of lymph transit times from hand to axilla ($t_{transit}$) in the same three healthy subjects in the absence and presence of pressure occlusion

Subject	$t_{transit}$ without cuff (min)	$t_{transit}$ with cuff (min)	Increase in $t_{transit}$ with cuff (-fold)	P_{pump} (mmHg)
A	3	42	14.0	50
B	6	63	10.5	30
C	6	33	5.5	50
Mean	5	46	10.0	43

The pressure cuff around the upper arm was initially at 60 mmHg for 30 min, then reduced in steps (see Cuffed protocol, Methods). Corresponding estimate of lymphatic pumping pressure, P_{pump}, also shown.

arrival of counts in the axillary ROI (ROI 3), $t_{transit}$, was 9.6 ± 7.2 min (3–21 min). On the basis of these results the duration of the initial occluding cuff pressure ($P_{cuff} = 60$ mmHg) in the cuffed protocol was set to 30 min, i.e. longer than maximum $t_{transit}$. Thus the absence of axillary radiolabel after 30 min in cuffed studies was not simply due to the transport distance, but indicated obstructed lymph flow.

Lymph transit in cuffed studies; total obstruction of lymph drainage by highest cuff pressure

The measurement of lymphatic pump force depended critically on the successful blockage of lymph flow at times longer than $t_{transit}$ (see Methods). To check this, $t_{transit}$ was measured in both free-draining, uncuffed studies and obstructive, cuffed studies in the same three normal subjects (2 male, 1 female, Table 3). Under free draining conditions these subjects had a $t_{transit}$ of 5.0 ± 1.7 min. With the cuff at 60 mmHg, no radiolabel reached the axilla by 30 min. Instead, longitudinal tracks of ^{99m}Tc-HIG-filled lymphatics distal to the cuff became broader with time, especially at the distal border of the cuff, indicating the accumulation of dammed lymph at this point (Figs 2 and 3). Transit under the cuff only occurred at 46 ± 15 min, after P_{cuff} had been reduced to 30–50 mmHg (Table 3).

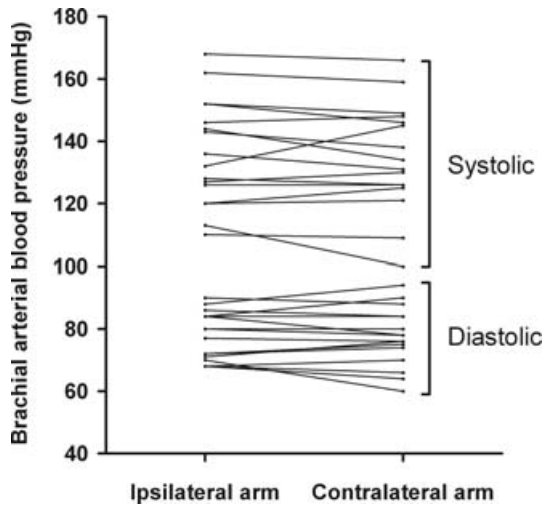

Figure 4. Paired measurements of diastolic and systolic brachial arterial blood pressure in ipsilateral (swollen) and contralateral arms of BCRL patients
Swollen arm arterial pressures, $136 \pm 17/78 \pm 8$ mmHg (systolic/diastolic), were almost identical to contralateral, non-swollen arm, $135 \pm 17/77 \pm 9$ mmHg. Swelling did not significantly impair pressure transmission from the occluding cuff to the deep tissues.

Comparison of P_{pump} in normal *versus* lymphoedematous arms

The measurement of P_{pump}, the lymphatic pumping pressure that overcame the occlusion cuff pressure, is illustrated in Fig. 2 for a normal subject with a high P_{pump}, 50 mmHg, and in Fig. 3 for the swollen arm of a BCRL patient (no. 15, Table 1) with a low P_{pump}, 10 mmHg. As the cuff pressure was reduced, a pressure was reached at which all normal subjects showed a clear, count-filled lymphatic vessel passing under the cuff. This pressure, P_{pump}, averaged 39 ± 14 mmHg (10–60 mmHg, $n = 16$) in healthy arms, with no significant difference between men (42 ± 11 mmHg, $n = 5$) and women (37 ± 15 mmHg; $P = 0.54$, $n = 11$, Student's unpaired t test).

As cuff pressure was reduced in lymphoedematous arms, lymphatic vessels filled under the cuff in eight cases; most showed extension of the dermal backflow pattern (see below) under the cuff. P_{pump} was significantly impaired in the swollen arms and averaged 24 ± 19 mmHg (0–60 mmHg, $n = 16$) ($P = 0.014$, Student's unpaired t test) (Fig. 5*A*). Moreover, there was a significant negative correlation between P_{pump} and the severity of ipsilateral forearm swelling; the weaker the pump, the more swollen was the forearm (Fig. 5*B*). The relation was described by the equation $100 \times \Delta V/V = [-0.68 \pm 0.23]P_{pump} + [49.4 \pm 6.9]$ (mean $\pm$ standard error of mean), where $100 \times \Delta V/V$ is the percentage increase in forearm volume relative to the opposite forearm ($100 \times$ difference between forearm volumes/contralateral forearm volume) and P_{pump} is in mmHg ($r = -0.62$, $P = 0.011$, $n = 16$). There was no significant correlation between P_{pump} and duration of swelling, whole arm swelling, hand swelling, age or body mass index.

Both groups showed a wide spread of pump values, with coefficients of variation of 35.1% and 78.2% for normal and lymphoedematous arms, respectively. In normal subjects, however, all but two (88%) had P_{pump} values of 30 mmHg or more and none was zero; whereas in lymphoedematous arms 50% had a P_{pump} of less than 30 mmHg and four had a P_{pump} of 0 mmHg (patients 1, 6,

13 and 16, Table 1). Of the latter, counts reached the axilla at 108 min in one case (6), reached the cuff but not axilla by 120 min in two cases (1, 16), and did not even reach the cuff in the fourth case (13). If the latter case is removed from the analysis, the depression of P_{pump} in BCRL remains significant ($P = 0.026$, $n = 15$ and 16, Student's unpaired t test). As might be expected from the above results, the residual depot counts after 120 min tended to be lower in the normal subjects ($47 \pm 17\%$, $n = 16$) than in BCRL patients ($52 \pm 15\%$, $n = 16$), though the difference was not statistically significant ($P = 0.35$, Student's unpaired t test).

P_{pump} in dominant (mainly right) BCRL arms (22.5 ± 18.3 mmHg) did not differ from P_{pump} in non-dominant (mainly left) BCRL arms (25.0 ± 20.0 mmHg; $P = 0.80$, $n = 8$ and 8, Student's unpaired t test).

Comparison of lymph velocities in uncuffed, cuffed normal and cuffed lymphoedematous arms

As noted earlier the average lymph tracer velocity in uncuffed normal arms was 8.9 ± 5.8 cm min^{-1} ($n = 7$). In the cuffed normal arms during the period at 60 mmHg, the initial tracer velocity from hand to distal cuff border was not significantly different, 7.6 ± 10.5 cm min^{-1} ($P = 0.34$, $n = 16$, unpaired t test). The corresponding initial velocity in the swollen arms was reduced to 3.2 ± 8.9 cm min^{-1} or 42% of the normal cuffed arm value ($P = 0.004$, $n = 16$, Student's unpaired t test). Lymphoedema was thus associated with reduced lymph velocity as well as reduced pump force.

Dermal backflow in lymphoedematous arms

In a normal arm the radiolabelled macromolecules delineate a small number of discrete, linear lymphatic pathways, whereas in many forms of lymphoedema there is often a diffuse filling of a network of fine dermal lymphatics, indicating a diversion or re-routing of the lymph from obstructed/failing main lymphatics (Stanton *et al.* 2001). This phenomenon, called 'dermal backflow', was evident in 15 of the 16 BCRL patients, including the patient of Fig. 3. A collector lymphatic vessel passing under the pressure cuff was clearly imaged in eight patients in addition to the dermal backflow distal to the cuff. Clearly imaged sub-cuff vessels were not unique to those with the least swelling or highest P_{pump}.

Biphasic rate of radiolabel accumulation in blood of uncuffed and cuffed healthy subjects

Blood was sampled from 6 of 7 uncuffed subjects and 13 of 16 cuffed normal subjects, in the belief that the sudden arrival of counts in the blood pool would provide a second, independent marker of sub-cuff lymph transmission and lymph flow. The results proved more complex, however, as follows.

Irrespective of cuffing, the blood counts slightly exceeded the background level from the first blood sample onwards, i.e. from 2 min post-injection, and were statistically significantly increased by 9 min (uncuffed, $P = 0.02$, $n = 6$, one sample t test) to 13 min (cuffed,

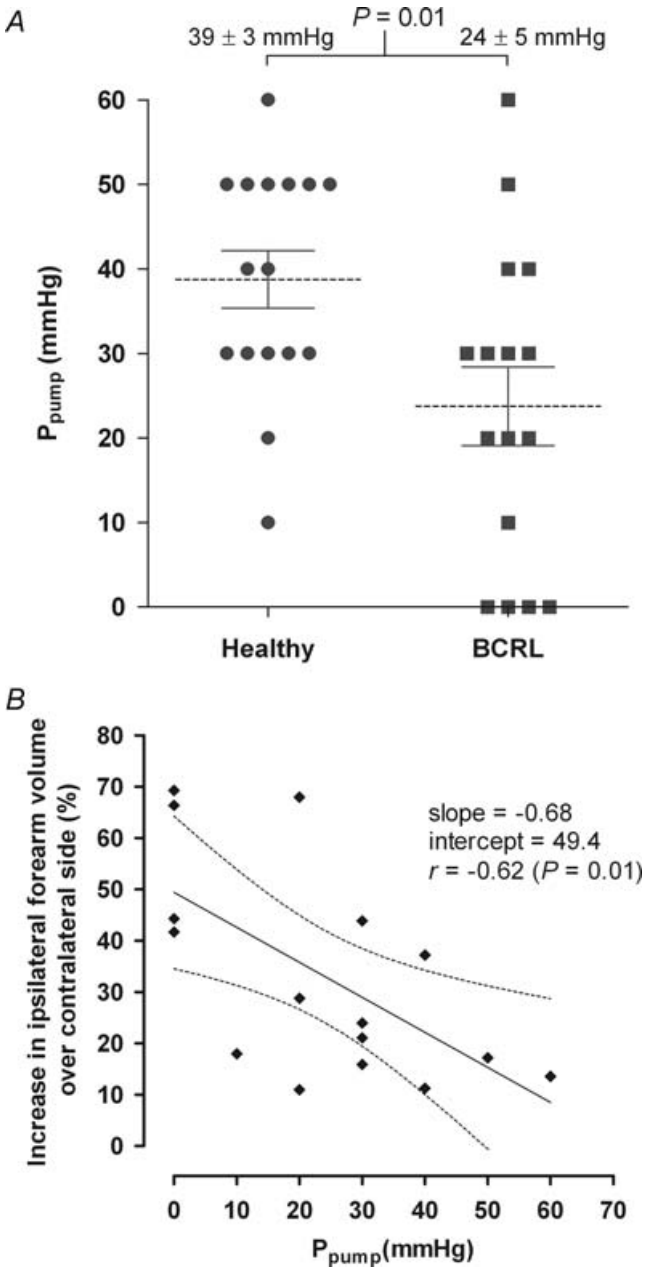

Figure 5. P_{pump} in normal arms and lymphoedematous arms
A, distribution, with mean and standard error bars. P_{pump} in lymphoedematous arms was significantly lower than in normal subjects. *B*, relation between percentage increase in swollen forearm volume and P_{pump}. Regression line with 95% confidence intervals shown.

$P = 0.04$, $n = 13$) (Fig. 6). There was thus a very early, albeit very small ($\leq 1\%$), entry of radiolabel into the blood of normal cuffed subjects long before any detectable tracer passed under the cuff (> 30 min). This raised the issue of direct diffusion of free label into dermal blood capillaries (see below).

The blood level increased biphasically, but with different timings in uncuffed and cuffed subjects. In the first, slow phase (2–120 min uncuffed, 2–60 min cuffed) the vascular accumulation rate J_{tracer} was low. Even in the uncuffed group it was only 0.016 ± 0.008 %AD min^{-1}, where %AD is the percentage of the administered depot dose (mean of regression slopes). J_{tracer} in the cuffed group at 2–60 min was not significantly different, 0.011 ± 0.001 %AD min^{-1} ($P = 0.29$, $n = 6$ and 13, Student's unpaired t test).

The start of the second, more rapid phase coincided, in the case of uncuffed subjects, with the subject standing up and walking to the waiting area to sit at ~130 min. At this point there was a sharp rise in J_{tracer} to 0.099 ± 0.042 %AD min^{-1} at 120–180 min. At the start of this phase 2.15 ± 0.92 % of the depot dose was in the blood pool and by 180 min this had increased to 8.75 ± 3.50 %.

Surprisingly, the second, rapid phase began earlier in cuffed than uncuffed subjects, at ~77 min, and occurred soon after the radiolabel had passed under the cuff, while the subject was still supine and stationary. The time at which tracer passed under the cuff (t_{cuff}, 55.7 ± 20.3 min for all 16 subjects; 52.8 ± 17.3 min for 13 subjects with blood samples) always preceded the time at which blood activity began to increase steeply (t_{blood}, 76.7 ± 14.9 min, $n = 13$) (Fig. 6). Moreover, the two values correlated significantly ($r = 0.66$, $P = 0.014$). The mean of the differences, 22.2 ± 12.9 min ($n = 13$), provided a measure of the transit time from the cuff to the lymphovenous junction in the neck plus circulation time, with an uncertainty of 5–10 min arising from the blood sampling frequency. J_{tracer} increased ~9-fold after the transit interval, to 0.095 ± 0.022 %AD min^{-1} at 70–120 min and 0.098 ± 0.027 %AD min^{-1} at > 120 min, the free movement period ($n = 13$). Movement at > 120 min did not increase J_{tracer} further in these subjects, even though the cuff was removed. By 180 min 12.3 ± 3.6 %AD was in the blood pool, an amount not significantly different from that in uncuffed subjects ($P = 0.48$, Student's unpaired t test).

Biphasic accumulation of radiolabel in blood of lymphoedema patients

The blood accumulation curve was again biphasic in BCRL patients. During the early, slow phase (2–60 min), the radiolabel reached statistically significant levels very early (11 min), long before the lymph transit time ($P < 0.001$, $n = 15$, one sample t test), as in the normal subjects (Fig. 6). J_{tracer} at 2–60 min, 0.016 ± 0.0004 %AD min^{-1}, was not significantly different from that of normal, cuffed subjects ($P = 0.54$, Student's unpaired t test).

The onset of the second, more rapid phase was very variable in BCRL patients. At 60–120 min J_{tracer} (0.025 ± 0.002 %AD min^{-1}) was less steep than in normal

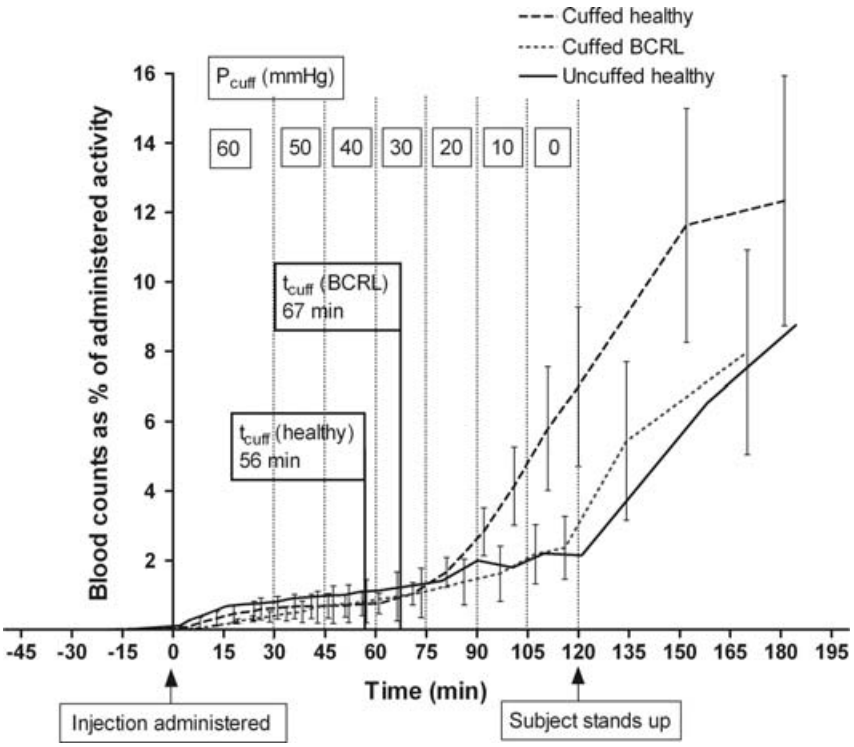

Figure 6. Blood radiolabel content *versus* time in uncuffed (continuous line) and cuffed (long-dashed line) normal subjects and cuffed BCRL patients (short-dashed line)
Values are means ± standard error of the mean (error bars for uncuffed subjects omitted for clarity). Subjects supine and stationary to 120 min post-injection, and then ambulant to 180 min. P_{cuff} is marked for each time interval between the vertical lines (not applicable to uncuffed subjects). t_{cuff}, the average time at which tracer passed under the cuff, is indicated for each of the cuffed groups.

cuffed subjects (0.095 ± 0.022 %AD min^{-1}), as might be expected from the impairment of lymph transmission under the congesting cuff in BCRL ($P = 0.03$, Student's unpaired t test). In the 12 patients where tracer eventually passed under the cuff and blood was sampled, t_{cuff} was 66.7 ± 25.6 min but this was followed by a sharp increase in J_{tracer} (second phase) in only 5/12 cases ($t_{cuff} = 63.6 \pm 34.1$ min, $t_{blood} = 73.0 \pm 14.6$ min, $n = 5$). The time lag in these patients was not significantly different from controls ($P = 0.13$, Student's unpaired t test), despite the axillary surgery. The sharp increase in J_{tracer} was not specific to those with dermal backflow as opposed to clearly delineated sub-cuff vessels.

As with uncuffed, normal subjects, the biggest increase in J_{tracer} (> 2-fold) occurred after 120 min, the cuff now removed and the patient having stood up to go and sit in the waiting area. In the 12 BCRL subjects where ^{99m}Tc-HIG reached the axilla, J_{tracer} increased to 0.076 ± 0.024 %AD min^{-1} at 120–180 min, compared with 0.033 ± 0.007 %AD min^{-1} during the stationary 2–120 min period ($P = 0.04$, two-way ANOVA). The blood counts reached 8.0 ± 2.9 %AD at 180 min – numerically less than in cuffed healthy subjects but not significantly so ($P = 0.22$), and no less than in normal uncuffed subjects.

Low molecular weight radiolabel *versus* protein-bound radiolabel in blood

In three BCRL patients the ^{99m}Tc-HIG failed to reach the axilla by 120 min (see earlier) yet 5.7 ± 4.6 % (1.1–6.9 %) of the depot radioactivity had accumulated in the blood pool. This reinforces the implication of the early, slow phase of J_{tracer}, namely that some radiolabel must enter the blood via a peripheral route, whether as intact ^{99m}Tc-HIG or as proteolysis fragments or as dissociated free ^{99m}Tc. The non-protein-bound fraction of radiolabel in the blood was therefore assessed by TCA precipitation (see Methods) in blood samples taken from six healthy subjects at 2, 91 and 184 min post-injection (BCRL blood not studied). All samples, and especially the first, showed a high percentage of 'free' (i.e. non-precipitated) ^{99m}Tc, namely 46–26 %. At 2 min post-injection, the protein-bound radioactivity was 54 ± 16 % (41–85 %), at 91 min 59 ± 13 % (51–76 %) and at 184 min 74 ± 13 % (64–89 %). The percentage of low molecular weight radiolabel in the blood therefore decreased with time ($P = 0.04$, one-way analysis of variance), in keeping with the diffusion of small solutes across capillaries and renal clearance. The total amount of free label in blood (as a percentage of the amount of free label injected in the original depot) was only 1.2 % at 2 min, 18.7 % at 91 min, and 33.1 % at 184 min. The values take no account, however, of any free label that has diffused into the interstitial compartment.

Discussion

Using a new, essentially non-invasive technique to quantify lymphatic collector pump force in human arms, the principal findings were that the hand-to-axilla lymph transit time is normally ~10 min; that a congesting cuff at 60 mmHg for 30 min arrests the lymph flow; that healthy arm lymphatics can pump hard enough to generate a pressure of ~39 mmHg; that lymphatics in the lymphoedematous arm show a fall in pumping force that is proportional to the severity of the swelling; and that blood radiolabel counts are an unsatisfactory index of lymphatic function following intradermal ^{99m}Tc-HIG injection in this particular experimental context. Overall the results supported the hypothesis of lymphatic pump failure in BCRL.

Assessment of new lymphatic congestion method; comparison with previous work

There are no previous, quantitative lymphoedema results for comparison, and just two results for normal human limbs. In obstructed human leg lymphatic collectors the lymph systolic pressure climbs to 37 mmHg, though with a wide range (2–55 mmHg) (Olszewski & Engeset, 1980). In the normal human arm a bandage pressure of 40–70 mmHg is required to prevent lymph flow from the wrist to the axilla (Howarth *et al.* 1994). The present results for normal arms (mean P_{pump} 39 mmHg, range 10–60 mmHg) are thus similar to the limited, existing data. The wide range of values is notable in both the present and previous work. In particular, 2/16 normal arms had a P_{pump} of only 10 mmHg and 20 mmHg, respectively.

It seems unlikely that the fall in P_{pump} in lymphoedematous arms is a methodological artefact, arising from the dissipation of sub-cuff pressure by an enlarged arm, for several reasons. First, the bilateral blood pressure measurements with appropriately tailored cuffs (Table 2) showed that the transmission of occlusive pressure to the deep tissue was equally effective in the swollen and contralateral arm. Second, impaired pressure transmission in swollen arms should artefactually raise, not lower, the estimate of P_{pump}, whereas the biggest arms actually had the lowest P_{pump} values. Third, the fall in the initial linear velocity of lymph between hand and cuff in BCRL was consistent with reduced lymphatic collector vessel contractility, although lymphatic distension may also contribute to this; and increases in cross-sectional area will reduce the velocity for a given volume flow. Fourth, not only P_{pump} but also the lymph drainage rate constant in BCRL muscle correlates negatively with the degree of arm swelling (Stanton *et al.* 2003).

The lymphatic congestion method inevitably caused venous congestion too, though blood flow was preserved by keeping the congestion pressure below diastolic

arterial pressure. Venous congestion raises capillary filtration pressure and thus ensures ample filtration for the generation of lymph (Stanton *et al.* 1999*a*). High local venous pressures should also reduce the likelihood of the direct flow of lymph through any peripheral lymphovenous anastomoses (see below). Venous congestion did not affect the early vascular accumulation of tracer, since J_{tracer} in cuffed healthy subjects at 60 mmHg cuff pressure was not significantly different from that in uncuffed healthy subjects over the same period (0–30 min).

The arms of normal subjects were used as controls rather than the contralateral arms of the BCRL patients because, in addition to practical considerations such as patient compliance and radiation dose, the contralateral arm of BCRL patients may differ from those of the general population in certain parameters (Mellor *et al.* 2000) or be affected indirectly by the disease process or treatment. Lymph flow normally correlates well between the two arms (Pain *et al.* 2003).

Lymph velocity in normal arm

The high uncuffed lymph velocity ($\sim$9 cm min^{-1}) and rapid hand–axilla transit ($<$ 3 min in some cases, mean 9.6 min) reinforced the finding of Ohtake & Matsui (1985) that radiolabel traverses normal arms and legs in 2–6 min. The reduction in lymph velocity from hand to occluding cuff is attributed to back-pressure from the occlusion site. Previous reports of lymph flow velocity have been limited to the mouse tail and human skin microlymphatics, based on fluorescence microlymphography. Leu *et al.* (1994) reported very low capillary lymph velocities in mice, 0.05 ± 0.04 cm min^{-1} (0.01–0.12 cm min^{-1}). In the dorsum of the supine human foot, Fischer *et al.* 1996) reported a median velocity of 3.1 cm min^{-1} (1.6 cm min^{-1} and 3.7 cm min^{-1} for lower and upper quartiles, respectively) during initial network filling. Intradermal colloid depots are cleared almost three times faster than adjacent subcutaneous depots (O'Mahony *et al.* 2004), probably due to the high lymphatic density and depot pressure in the dermis (Hudack & McMaster, 1933; Mortimer *et al.* 1990; Stanton *et al.* 1999*b*; Mellor *et al.* 2000). The intradermal route was thus ideally suited for γ-camera imaging of the lymphatics.

Pump force in normal arm; practical importance

As discussed above, previous estimates of normal human leg and arm lymphatic pumping indicated P_{pump} values similar to the present finding of 39 mmHg (10–60 mmHg). The upper limit of the P_{pump} range is of practical value, because it defines the compression pressure that should be applied, ideally, to cases of snake or spider envenomation of the hand or arm. Also, the transit time results show that lymphatic compression needs to be applied quickly, in no more than 10 min and preferably $<$ 3 min, if lymphatic drainage is to be prevented effectively.

Pump force in lymphoedema; lymphatic failure

This is the first report, to our knowledge, of lymphatic contractile force in lymphoedema, and the finding of a reduced P_{pump} supports the hypothesis that lymphatic contractile failure contributes to the pathogenesis of lymphoedema, cf. simple stopcock hypothesis. This conclusion is greatly strengthened by the significant negative relation between P_{pump} and degree of swelling; the lower the lymphatic pump force, the greater the percentage swelling of the arm. The reduction in P_{pump} by 38 % in BCRL patients with 32 % mean swelling is comparable in magnitude with the reduction in muscle lymph drainage rate by 31 % in patients with 34 % mean swelling (Stanton *et al.* 2003). We suggest that the lymphatic pump failure is analogous to cardiac failure following a chronically raised afterload, such as essential hypertension. Lymphatic afterload is probably increased by the raised outflow resistance created by damage to the axillary lymphatic system during surgery and radiotherapy.

Lymphatics isolated from chronic lymphoedematous tissue have never been studied directly, but isolated bovine lymphatics show a fall in lymphatic stroke volume and output at transmural pressures of $>$ 8.4 mmHg, despite increased frequency of contractions (McHale & Roddie, 1983). Lymphatics in conscious sheep tolerate higher transmural pressures, 13–19 mmHg, before onset of lymphatic failure (McGeown *et al.* 1987). The contribution of duration of a moderately raised, chronic afterload on lymphatic failure has not been studied.

Impaired lymphatic contractility is probably not the sole factor responsible for swelling, however, since two BCRL patients, albeit with below-average percentage swelling, had good P_{pump} values (50–60 mmHg). Furthermore, since only a minority of women develop BCRL after breast cancer treatment and some women who have had just one axillary lymph node removed develop BCRL whereas others who have had axillary clearance surgery do not develop BCRL, it is tempting to speculate that the subclass of arms that normally have low P_{pump} values might form an oedema-prone subgroup. This hypothesis is supported by evidence for lymphatic abnormalities in the *contralateral* arm of women with BCRL. Dermal lymphatic vessels in the contralateral forearm of BCRL patients are abnormally wide compared with lymphatics in the arms of matched breast cancer patients without BCRL (Mellor *et al.* 2000), and the lymph drainage rate constant for ^{99m}Tc-HIG in the subcutis of contralateral hand of BCRL patients with swollen hands is increased relative to the hands of BCRL patients with hand-sparing (Stanton *et al.*

2006). It is possible that some women are constitutionally (genetically) predisposed to BCRL after breast cancer treatment by having less robust lymph drainage or high filtration rates prior to surgery.

Interpretation of early arrival of blood radiotracer

It was hoped that the first appearance of blood counts would mark the arrival of radiolabelled lymph in the blood pool, but low levels of radiolabel (< 1 % administered dose) appeared in blood within a few minutes of injection, long before any lymph reached the axilla even in the absence of a cuff. Early radiolabel in the blood pool was seen in cuffed normal subjects, cuffed BCRL patients, and even three BCRL patients in whom ^{99m}Tc-HIG failed to reach the axilla by 120 min. This indicated a small, local entry of ^{99m}Tc or ^{99m}Tc-HIG into the peripheral bloodstream of the arm. Part of the vascular uptake can be attributed to the small amount of free radiolabel in the preparation (≤ 5 %), but this may not be the full explanation since the TCA precipitation studies showed that nearly half the early blood counts were protein-bound. Further work is needed to establish whether the bound counts represented spontaneous binding of free ^{99m}Tc to circulating plasma proteins or whether they bound to HIG that gained direct, local entry into the arm circulation, either by vesicular transport across microvascular endothelium or through minor lymphovenous anastomoses (Aboul-Enein *et al.* 1984; Schmid-Schönbein, 1990; Modi *et al.* 2007).

It is difficult to see how a small, limited mass of free label in the injectate could maintain the blood level, because free label quickly diffuses out of the circulation (unless it binds to circulating plasma proteins). Pilot dialysis study results indicated a low rate of spontaneous dissociation of ^{99m}Tc-HIG *in vitro* but only sufficient to account for < 8 % of the observed J_{tracer}. It is conceivable that production of diffusible radiolabel might be accelerated *in vivo*, for example by proteolysis (Casley-Smith & Casley-Smith, 1985, Casley-Smith *et al.* 1993).

Interpretation of later increases in blood radiotracer accumulation rate

At > 30 min the pattern of blood radiolabel accumulation differed between cuffed and uncuffed normal arms; and between cuffed normal and cuffed BCRL arms. In cuffed normal arms, there was a sharp increase in J_{tracer} soon after lymph passed the congesting cuff, due to the drainage of labelled lymph into the neck veins. In BCRL arms the increase was much less marked or even absent, in keeping with impaired lymph flow. In uncuffed subjects, the most pronounced increase in J_{tracer} occurred when the patient stood up and moved around, indicating that movement or orthostasis increased arm lymph flow. This was also prominent in the BCRL patients, and could be due to the well-documented passive transport of lymph by tissue movement, including extrinsic pumping by skeletal muscle movement (Taylor *et al.* 1957; Garlick & Renkin, 1970; McGeown *et al.* 1987). It could also be due to an orthostatic effect on intrinsic lymphatic contraction frequency (Olszewski & Engeset, 1980), possibly as a sympathetically mediated reflex. Since J_{tracer} had already reached high values prior to movement/orthostasis in the cuffed normal arms, it appears that lymphatic congestion had already maximally stimulated the lymphatic pump.

Conclusions

The lymphatic congestion lymphoscintigraphy method enabled non-invasive, quantitative estimation of lymphatic contractility in normal humans and patients with lymphoedema. The results showed a fall in lymphatic collector pump force that was proportional to the degree of oedema in BCRL. The findings thus supported the hypothesis that chronic afterload elevation leads to lymphatic failure, analogous to hypertensive cardiac failure, and that this contributes to (but probably does not fully explain) the pathogenesis of lymphoedema. The lymphatic failure hypothesis has the potential to explain both the spatial and temporal heterogeneity of BCRL. It also raises the possibility of investigating pharmacological therapies for lymphatic failure.

References

Aboul-Enein A, Eshmawy I, Arafa MS & Abboud A (1984). The role of lymphovenous communication in the development of postmastectomy lymphedema. *Surgery* **95**, 562–565.

Andrews JT & Milne MJ (1977). *Nuclear Medicine: Clinical and Technological Bases*. Wiley, New York.

Blanchard DK, Donohue JH, Reynolds C & Grant CS (2003). Relapse and morbidity in patients undergoing sentinel node biopsy alone or with axillary dissection for breast cancer. *Arch Surg* **138**, 482–487.

Casley-Smith JR & Casley-Smith JR (1985). The effect of calcium dobesilate on acute lymphoedema (with and without macrophages) and on burn oedema. *Lymphology* **18**, 37–45.

Casley-Smith JR, Morgan RG & Piller NB (1993). Treatment of lymphedema of the arms and legs with 5,6-benzo-[α]-pyrone. *New Engl J Med* **329**, 1158–1163.

Clodius L (1977). Secondary arm lymphoedema. In *Lymphedema*, ed. Clodius L, pp. 147–174. Georg Thieme, Stuttgart.

Feldman MG, Kohan P, Edelman S & Jacobson JH (1966). Lymphangiographic studies in obstructive lymphedema of the upper extremity. *Surgery* **59**, 935–943.

Fischer M, Franzeck UK, Herrig I, Ostanzo U, Wen S, Schiesser M, Hoffmann U & Bollinger A (1996). Flow velocity of single lymphatic capillaries in human skin. *Am J Physiol Heart Circ Physiol* **270**, H358–H363.

Garlick DG & Renkin EM (1970). Transport of large macromolecules from plasma to interstitial fluid and lymph in dogs. *Am J Physiol* **219**, 1595–1605.

Hack TF, Cohen L, Katz J, Robson LS & Goss P (1999). Physical and psychological morbidity after axillary lymph node dissection for breast cancer. *J Clin Oncol* **17**, 143–149.

Halsted WS (1921). The swelling of the arm after operations for cancer of the breast-elephantiasis chirurgica – its cause and prevention. *Bull John Hopkins Hosp* **32**, 309–313.

Howarth DM, Southee AE & Whyte IM (1994). Lymphatic flow rates and first-aid in simulated peripheral snake or spider envenomation. *Med J Aust* **161**, 695–700.

Hudack SS & McMaster PD (1933). The lymphatic participation in human cutaneous phenomena. A study of the minute lymphatics of the skin. *J Exp Med* **57**, 751–774.

Leu AJ, Berk DA, Yuan F & Jain RK (1994). Flow velocity in the superficial lymphatic network of the mouse tail. *Am J Physiol Heart Circ Physiol* **267**, H1507–H1513.

Levick JR & McHale NG (2002). Physiology of lymph production and propulsion. In *Diseases of the Lymphatics*, ed. Browse N, Burnand KG & Mortimer PS, pp. 44–65. Arnold, London.

McGeown JG, McHale NG & Thornbury KD (1987). The role of external compression and movement in lymph propulsion in the sheep hindlimb. *J Physiol* **387**, 83–93.

McHale NG & Roddie IC (1983). The effects of catecholamines on pumping activity in isolated bovine mesenteric lymphatics. *J Physiol* **338**, 527–536.

Mansel RE, Fallowfield L, Kissin M, Goyal A, Newcombe RG, Dixon JM, Yiangou C, Horgan K, Bundred N, Monypenny I, England D, Sibbering M, Abdullah TI, Barr L, Chetty U, Sinnett DH, Fleissig A, Clarke D & Ell PJ (2006). Randomized multicenter trial of sentinel node biopsy versus standard axillary treatment in operable breast cancer: The ALMANAC trial. *J Natl Cancer Inst* **98**, 599–609.

Mellor RH & Mortimer PS (2004). Dermal lymphatics. In *Measuring the Skin*, ed. Agache P & Humbert P, pp. 392–398. Springer, Berlin.

Mellor RH, Stanton AWB, Azarbod P, Sherman MD, Levick JR & Mortimer PS (2000). Enhanced cutaneous lymphatic network in the forearms of women with postmastectomy oedema. *J Vasc Res* **37**, 501–512.

Modi S, Stanton AWB, Mellor RH, Peters AM, Levick JR & Mortimer PS (2005). Regional distribution of epifascial swelling and epifascial lymph drainage rate constants in breast cancer related lymphedema. *Lymphat Res Biol* **3**, 3–14.

Modi S, Stanton AWB, Mortimer PS & Levick JR (2007). Clinical assessment of human lymph flow using removal rate constants of interstitial macromolecules: a critical review of lymphoscintigraphy. *Lymphat Res Biol* **5** (in press).

Mortimer PS, Bates DO, Brassington HD, Stanton AWB, Strachan DP & Levick JR (1996). The prevalence of arm oedema following treatment for breast cancer. *Q J Med* **89**, 377–380.

Mortimer PS, Simmonds R, Rezvani M, Robbins ME, Hopewell JW & Ryan TJ (1990). Measurement of skin lymph flow by an isotope clearance technique: reliability, reproducibility. Effect of injection dynamics and lymph flow enhancement. *J Invest Dermatol* **95**, 677–682.

Ohtake E & Matsui K (1985). Lymphoscintigraphy in patients with lymphoedema. A new approach using intradermal injections of technetium-99m human serum albumin. *Clin Nucl Med* **11**, 474–478.

Olszewski WL & Engeset A (1980). Intrinsic contractility of prenodal lymph vessels and lymph flow in human leg. *Am J Physiol Heart Circ Physiol* **239**, H775–H783.

O'Mahony S, Rose SL, Chilvers AJ, Ballinger JR, Solanki CK, Barber RW, Mortimer PS, Purushotham AD & Peters AM (2004). Finding an optimal method for imaging vessels of the upper limb. *Eur J Nucl Med Mol Imaging* **31**, 555–563.

Pain SJ, Barber RW, Ballinger JR, Solanki CK, Mortimer PS, Purushotham AD & Peters AM (2004*a*). Local vascular access of radioprotein injected subcutaneously in healthy subjects and patients with breast cancer-related lymphoedema. *J Nucl Med* **45**, 789–796.

Pain SJ, Barber RW, Ballinger JR, Solanki CK, Mortimer PS, Purushotham AD & Peters AM (2004*b*). Tissue-to-blood transport of radiolabelled immunoglobulin injected into the web spaces of the hands of normal subjects and patients with breast cancer-related lymphoedema. *J Vasc Res* **41**, 183–192.

Pain SJ, Barber RW, Ballinger JR, Solanki C, O'Mahony S, Mortimer PS, Purushotham A & Peters AM (2003). Side-to-side symmetry of radioprotein transfer from tissue space to systemic vasculature following subcutaneous injection in normal subjects and patients with breast cancer. *Eur J Nucl Med Mol Imaging* **30**, 657–661.

Pain SJ, Nicholas RS, Barber RW, Ballinger JR, Purushotham AD & Peters AM (2002). Quantification of lymphatic function for investigation of lymphoedema: depot clearance and rate of appearance in blood of soluble macromolecules. *J Nucl Med* **43**, 318–324.

Schmid-Schönbein GW (1990). Microlymphatics and lymph flow. *Physiol Rev* **70**, 987–1028.

Schunemann H & Willich N (1997). Lymphodeme nach mammakarzinom. Eine studie uber 5868 falle. *Dtsch Med Wochenschr* **122**, 536–541.

Stanton AWB, Badger C & Sitzia J (2000). Non-invasive assessment of the lymphedematous limb. *Lymphology* **33**, 122–135.

Stanton AWB, Holroyd B, Mortimer PS & Levick JR (1999*a*). Comparison of microvascular filtration in human arms with and without postmastectomy oedema. *Exp Physiol* **84**, 405–419.

Stanton AWB, Mellor RH, Cook GJ, Svensson WE, Peters AM, Levick JR & Mortimer PS (2003). Impairment of lymph drainage in subfascial compartment of forearm in breast cancer-related lymphoedema. *Lymphatic Res Biol* **1**, 121–132.

Stanton AWB, Modi S, Mellor RH, Peters AM, Svensson WE, Levick JR & Mortimer PS (2006). A quantitative lymphoscintigraphic evaluation of lymphatic function in the swollen hands of women with lymphoedema following breast cancer treatment. *Clin Sci* **110**, 553–561.

Stanton AWB, Northfield JW, Holroyd B, Mortimer PS & Levick JR (1997). Validation of an optoelectronic limb volumeter (Perometer). *Lymphology* **30**, 77–97.

Stanton AWB, Patel HS, Levick JR & Mortimer PS (1999*b*). Increased dermal lymphatic density in the human leg compared with the forearm. *Microvasc Res* **57**, 320–328.

Stanton AWB, Svensson WE, Mellor RH, Peters AM, Levick JR & Mortimer PS (2001). Differences in lymph drainage between swollen and non-swollen regions in arms with breast cancer-related lymphoedema. *Clin Sci* **101**, 131–140.

Stewart T & Treves N (1948). Lymphangiosarcoma in postmastectomy lymphoedema. *Cancer* **1**, 64–81.

Taylor GW, Kinmonth JB, Rollinson E, Rotblat J & Francis GE (1957). Lymphatic circulation studied with radioactive plasma protein. *Br Med J* **i**, 133–137.

Velanovich V & Szymanski W (1999). Quality of life of breast cancer patients with lymphoedema. *Am J Surg* **177**, 184–187.

Acknowledgements

The authors thank Dr A. Al-Nahhas, J. Murrell, D. Towey and colleagues, Nuclear Medicine, Hammersmith Hospital, London, for assistance with the lymphoscintigraphic studies; Dr A. Irwin, Dr S. Sassi, N. Gulliver, Physics, St George's Hospital, London, for assistance with image analysis and counting of blood samples; D. Lui, University College Hospital, London, for preparation of ^{99m}Tc-HIG; A. Wallace, Lymphoedema Support Network, for assistance with recruitment; A. C. Cossor & Son (Accoson) Ltd, London, for providing the blood pressure cuffs; and the participants. The research was supported by Wellcome Trust grant 063025.